

**Finite Element Analysis (FEA) on Friction Stir Welding of
Aluminium Alloy, AA5083 Using Coupled Eulerian-
Lagrangian Model with Time-Scaling**

by

Syahmi Bin Ismail

22739

Dissertation report submitted in partial fulfilment of
the requirements for the
Bachelor of Mechanical Engineering
With Honours

FYP 2

January 2020

Universiti Teknologi PETRONAS
32610 Seri Iskandar
Perak Darul Ridzuan

CERTIFICATION OF APPROVAL

Finite Element Analysis (FEA) on Friction Stir Welding of Aluminium Alloy, AA5083 Using Coupled Eulerian- Lagrangian Model with Time-Scaling

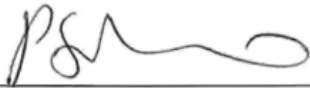
by

Syahmi Bin Ismail

22739

A project dissertation submitted to the
Mechanical Engineering Programme
Universiti Teknologi PETRONAS
in partial fulfilment of the requirement for the
BACHELOR OF MECHANICAL ENGINEERING
WITH HONOURS

Approved by,



(Assoc Prof Dr Srinivasa Rao Pedapati)

UNIVERSITI TEKNOLOGI PETRONAS
BANDAR SERI ISKANDAR, PERAK

January 2020

CERTIFICATION OF ORIGINALITY

This is to certify that I am responsible for the work submitted in this project, that the original work is my own except as specified in the references and acknowledgements, and that the original work contained herein have not been undertaken or done by unspecified sources or persons.



SYAHMI BIN ISMAIL

ABSTRACT

Friction stir welding (FSW) is a unique method of welding that can produce high quality of joint. There are various process parameters that can influence the quality which includes the welding speed, rotational speed, axial force, tool design, tool tilt angle, plunge depth, pin design, material and friction coefficient. Many researches have been conducted to study the effect of varying those parameters values to the quality of the welded joint. Based on the previous researches, the thermal-related parameters are the main contributors that affect the quality of the joint. There are two main approaches to conduct a research on FSW process; experimental and numerical simulation/analysis. Numerical analysis has proven to be more advantageous compare to experimental approaches due to its ability to discretize a model into smaller element to perform mathematical analysis. It has made the study of properties especially those properties that can distribute throughout a material such thermal distribution and stress distribution become simple with less time and cost. In this study, numerical analysis on FSW process via Finite Element Analysis (FEA) method was to be conducted by using Abaqus software. The model was developed based on Coupled Eulerian-Lagrangian approaches due to large deformation occurred during the FSW process. As the whole process to run the numerical analysis was time consuming, this study had proposed the possibilities of applying time-scaling in the simulation. The process would butt joint welding on aluminum alloy, AA5083 as the workpiece with welding speed of 16 mm/min, 28 mm/min and 40 mm/min and constant rotational speed of 500 rpm. The remaining parameters where kept constant. The proposed time-scaling method had significantly shortened the time required to perform the analysis and its feasibility would be verified based on the temperature distribution along the workpiece.

ACKNOWLEDGEMENT

Final Year Project (FYP) has given me an opportunity for to develop self-learning quality. Besides that, it also helps me to equip myself with the ability to conduct a research in proper way. For this project, I have been assigned to conduct a Finite Element Analysis (FEA) on the Aluminium Alloy, (AA 5083). The project has provided me with the advantages to learn and apply Abaqus for solving engineering related problems. With the extra knowledges FEA by using Abaqus, it has equipped me with some distinctive quality as an engineering student. All of the benefits cannot be achieved without the great supports to help me in conducting the project.

Therefore, I would like to express my deepest gratitude to my supervisor, Dr. Rao Srinivasa Pedapati for entrusting me with the project. He also provides some guidance to conduct the project. Besides that, we also have some constructive discussions on the ways or methods to enhance the project. I am very grateful to have a very good supervisor that has helped me a lot to complete the project.

Besides that, I would like to give the outmost gratitude to my parents and friends that have gave me the moral support needed to complete the project. I really appreciate the every single knowledge and contribution from them. Some of them are willing to put some efforts to understand my project in order to help me to deal with the problems.

Lastly, I also want to acknowledge Universiti Teknologi PETRONAS (UTP) for providing all the required facilities to conduct my project. It has provides computer laboratories that are equipped with various software. The laboratories are also very accommodating and comfortable. The students can utilize the laboratories to enhance their learning experiences.

Sincerely,

Syahmi

Table of Contents

CERTIFICATION OF APPROVAL	ii
ABSTRACT	iv
ACKNOWLEDGEMENT	v
List of Figures	viii
List of Tables	ix
CHAPTER 1: INTRODUCTION.....	1
1.1 Background	1
1.2 Problem Statement	3
1.3 Objectives	3
1.4 Scope of Study	4
1.5 Hypothesis.....	4
CHAPTER 2: LITERATURE REVIEW.....	5
2.1 Finite Element Analysis (FEA) for FSW Process Evaluation	5
2.2 Various FEA Modelling Methods on FSW Process	7
2.3 Finite Element Analysis (FEA) Softwares	8
2.4 Properties of Aluminium Alloy, AA5083.....	9
2.5 Johnson Cook Material Model.....	12
CHAPTER 3: METHADODOLOGY	14
3.1 FE Modelling Using Coupled Eulerian Lagrangian Method	14
3.2 Time Scaling Approach	22
3.3 Project Activities / Gantt Chart.....	27

CHAPTER 4: RESULT AND DISCUSSION.....	28
4.1 Estimated Heat Energy and Temperature	28
4.2 Graphical Result of FE Simulation for FSW Welding.....	31
4.3 Temperature Distribution along Z-axis.....	33
4.4 Result Validation	37
CHAPTER 5: CONCLUSION AND RECOMMENDATION	38
5.1 Conclusion	38
5.2 Recommendation	39
REFERENCES	40
APPENDICES	44

List of Figures

Figure 2.1 The strain-stress diagram of AA5083 at different temperature	11
Figure 3.1 The Model of Euler Plate, Reference Plate & Tool.....	14
Figure 3.2 The Assembly of the Models.....	15
Figure 3.3 Meshed Euler Plate and Tool.....	16
Figure 3.4 Relationship of Specific Heat Capacity of AA5083 and Temperature.....	24
Figure 3.5 Relationship of Thermal Conductivity of AA5083 and Temperature	25
Figure 3.6 Relationship of Density of AA5083 and Temperature	25
Figure 3.7 Relationship of Elasticity of AA5083 and Temperature	26
Figure 3.8 The gant chart of the project.....	27
Figure 4.1 FSW with Time-Scaling (500 RPM, 16 mm/min).....	31
Figure 4.2 FSW with Time-Scaling (500 RPM, 28 mm/min).....	32
Figure 4.3 FSW with Time-Scaling (500 RPM, 40 mm/min).....	32
Figure 4.4 Temperature Distribution of FSW Welding (500 rpm, 16 mm/min).....	34
Figure 4.5 Temperature Distribution of FSW Welding (500 rpm, 28 mm/min).....	34
Figure 4.6 Temperature Distribution of FSW Welding (500 rpm, 40 mm/min).....	34
Figure 4.7 Temperature Distribution of FSW Welding of both Simulation and Experimental on aluminium alloy, AA5083 (Welding Speed: 40mm/min, Rotational Speed: 500rpm)	37

List of Tables

Table 2.1 The chemical compositions of AA5083 and AA6061	9
Table 2.2 The temperature dependent properties of AA5083	10
Table 2.3 The temperature dependent mechanical properties of AA5083.....	10
Table 2.4 Johnson Cook Model Paramters for Aluminium Alloy, AA5083	13
Table 3.1 The Set of Unit Used in Abaqus	15
Table 3.2 The relationship of Tool rotational speed (TRS), Tool Speed (TS), Tool Tilt Angle (TTA) with the mechanical properties of AA5083	17
Table 3.3 Welding Transverse Speed and Rotational Speed Before Time-Scaling.....	23
Table 3.4 Welding Transverse Speed and Rotational Speed After Time-Scaling	23
Table 4.1 Theoretical Calculation for Heat Energy Created & Temperature of the Workpiece Based on Steady-State Conditions.....	30

CHAPTER 1

INTRODUCTION

1.1 Background

Friction Stir Welding (FSW) is a solid-state joining process that was invented by The Welding Institute (TWI) in December 1991 Thomas, Johnson, and Wiesner (2003). In contrast with the conventional welding, FSW welds the materials together without melting the base material which is the main reason it is called as solid-state joining process. It uses a non-consumable cylindrical shoulder tool with profile pin that will be rotated and plunged into the base materials. The rotation of the shoulder against the surface of the materials generates frictional heating to heat the tool-material interface area to a temperature below recrystallization temperature which will cause the softening of the material at the area, producing a continuous welded joint as the tools translating along the welding line (Thomas et al., 2003). Besides the frictional heat, there is also adiabatic heat generated within the material. As the tool move along the welding line, it mechanically intermixes and forges the hot and softened materials in the weld zone, much like joining clay or dough.

Early application of FSW is on aluminium alloy since it has low recrystallization temperature and considered as soft metal which caused less tool wear during the process. However, new development in material engineering has abled to create tools with high wear resistance that can be used in FSW for copper alloys, mild steel, stainless steel, magnesium alloy and even titanium alloy. In recent development, FSW has successfully welded high density polyethylene (HDPE) – carbon black deposited (Sheikh-Ahmad, Ali, Deveci, Almaskari, & Jarrar, 2019). It is breakthrough in welding process which previously only capable of welding metals. Besides that, FSW also able to welded joint with two different materials. (M. M. El-Sayed, Shash, & Abd-Rabou, 2018).

Since the FSW process requires no melting of the base materials, it can avoid the defects such as crack, thermal deformation, porosity and so on which are commonly happen in melting welding (Fei & Wu, 2018). Besides that, it also prevent the fusion of foreign atom or particles into the weld area, eliminating the need of shielding gas that has made this welding technique is considered as environmentally friendly. It also can to weld the 2xxx and 7xxx aluminum alloys which are difficult to weld by using conventional melting welding due to the poor solidification microstructure and the porosity in the fusion zone. Due to the advantages, FSW has become a critical technology in various industrial applications including aerospace, maritime, railway, automotive and space exploration.

Despite of the advantages, FSW also have some disadvantages. It left exit hole when the tool is withdrawn after the welding process completed. Besides that, it requires large down forces with heavy-duty clamping to hold the workpieces together during the process. As the FSW process performed by machine, it has less flexibility compare to manual conventional welding such as arc welding. Furthermore, the welding speed is slower compare to some fusion welding techniques although it might be compensate by fewer welding passes are required.

In term of the mechanical properties of the welded joint, FSW produces superior quality of joint. Jannet, Mathews, and Raja (2014) have conducted a study on the mechanical properties comparison between FSW and fusion welding (MIG & TIG). They has reported that the tensile strength of the FSW joint is superior compare to fusion welding. Besides that, they also found out that the hardness of the joints is almost similar for all the welding method. However, the hardness is relatively high at the weld region compare to the heat affected zone (HAZ). Furthermore, FSW welded joints produced better fatigue properties compare to fusion welding. The residual stress developed during the FSW process is lower compare to fusion welding which is due to lower temperatures involved in the process. In depth study needed to study the effect of welding parameters and the quality of joint. FEA modelling was the best approaches in

analyzing FSW process especially on stress distribution, temperature distribution and other parameters distributed in the workpiece. Therefore, a reliable modelling approach which could deliver accurate analysis with least resources (time & money) was required.

1.2 Problem Statement

Finite Element Analysis (FEA) is a numerical analysis that has been applied to study and understand FSW process in order to improve the quality of joint produced. It is a very powerful method to analyze properties that are distributed in a material such as temperature distribution, stress distribution and strain distribution. Several researchers have opted to model the FSW cycle in various models, such as analytical thermal models, finite element based solid thermal and thermos-mechanical and computational fluid dynamic models.(M. M. El-Sayed et al., 2018). Although this method has been found to be more superior compare to experimental method, sometimes its time consuming process does not compensate with the cost of performing the same analysis via experimental approach. This case happened to FEA analysis on FSW process. It is very time consuming to run the analysis. Although various modelling method available to perform the analysis; Coupled Eulerian-Lagrangian model, Arbitrary Lagrangian-Eulerian (ALE) model, and etc, they are still time consuming analysis. It is mainly due to high deformation that occurred during the process which required explicit analysis. Therefore, a special approach needed to be developed to solve the time constraint issue.

1.3 Objectives

There are few objectives need to be achieved throughout the study:

1. To develop a finite element model of FSW process based on Coupled Eulerian-Lagrangian model.
2. To propose the possibilities of time-scaling in the modelling to shorten the time for analysis.

1.4 Scope of Study

The scopes of the study are stated as below:

1. The study only focused on AA5083 (its properties and Johnson-Cook model)
2. The modelling was based on Coupled Eulerian-Lagrangian Method.
3. The feasibility of time-scaling would be studied and verified.
4. The study only interested in temperature distribution in the workpiece in other to verify the feasibility of time-scaling approaches.
5. The only manipulated variable in the study was welding speed; 16 mm/min, 28 mm/min and 40 mm/min.
6. All the necessary equations were obtained from external legitimate sources.
7. The remaining welding parameters; rotational speed, tool design, axial force, plunge depth and tool tilt angle were obtained from external legitimate sources and kept similar throughout the study.
8. The loss of heat generated to the surrounding due to convection and radiation are neglected.
9. The loss of heat generated to the contact between the bottom surface of the work piece and the backing plate are neglected.

1.5 Hypothesis

The study is conducted based on the hypothesis as stated below:

1. Increase in the rotational speed will produce finer grain and increase the residual stress.

CHAPTER 2

LITERATURE REVIEW

2.1 Finite Element Analysis (FEA) for FSW Process Evaluation

Finite element Analysis (FEA) on friction stir welding has been adopted by many researches as an alternative to experimental investigation. Experimental study on FSW is more complex due to its three-dimensional nature, costly and time consuming. Besides that, there is inaccuracy during the measurement of the data during the experimental study. Therefore, FEAs have become a common method used by researchers for FSW study as it can produce more accurate results compare to the experimental method. Sometimes, the researchers employed the method to complement their experimental studies.

Several researchers opted to model the FSW process in different kinds of model such as analytical thermal models, finite element based solid thermal and thermos-mechanical and computational fluid dynamic models (M. M. El-Sayed et al., 2018). Generally, the FSW modelling has been conducted to study the heat generation, thermal distribution, material flows at the weld zone and welding induced stress. Kiral, Tabanoglu, and Serindag (2013) have developed a 3D heat transfer finite element model using ANSYS and Hyper Extrude software to simulate the thermal distribution during the FSW of AA6061-T6. Besides that, Yaduwanshi, Bag, and Pal (2014) have developed a 3D heat flow numerical model to predict the heat generated from FSW process on aluminum alloys. (Buffa, Fratini, & Pasta, 2009) also have studied the residual stresses induced during the FSW process. Other than that, Mostafa M. El-Sayed, Shash, Mahmoud, and Rabbou (2018) have constructed a finite element model to simulate the peak temperature during FSW process of AA5083.

Several important parameters need to be considered in the FSW process which need to be considered throughout the Finite Element Analysis. The parameters are rotational speed of tools, welding speed, tool design, axial force, plunge depth and tool tilt angle (M. M. El-Sayed et al., 2018). These are the parameters that will affect the quality of welding joints especially in term of mechanical property. Chandrashekar, Reddappa, and Ajaykumar (2016) have investigated the relationship of the rotational speed and tool pin profile with the tensile properties of AA5083-H111. They stated that tool pin profile and rotational speed values from 600 rpm to 1000 rpm significantly affect the tensile strength of the welded joints. Tensile strength was increased with the increased in rotational speed in the case of triflute pin profile; while the tensile strength decreased with the increased in rotational speed in the case of tapered pin profile. Khodir, Shibayanagi, and Naka (2006) have studied the effect of rotational speed on the mechanical properties of AA2024-T3. They found out that the increase of rotational speed from 400 rpm to 1500 rpm resulted in increasing the grains size in the weld nugget, thus increasing its yield strength and tensile strength values. Besides that, Mao et al. (2015) have studied the relationship between the rotational and welding speed and microstructure evolution of AA2060, aluminum lithium alloy. They varied the rotational speed value from 750 rpm to 1500 rpm. They discover that the increase of the rotational speed from 750 rpm to 1180 rpm decreased the grains size in the weld nugget. However, the grains size increased at 1500 rpm. Meanwhile, the increase in welding speed from 95 mm/s to 150 mm/s resulted in the fluctuation of grains size. Furthermore, Lombard, Hattingh, Steuwer, and James (2009) have studied the affect rotational and welding speed on the residual stress profile of AA5083-H321. They found that the residual stress profiles are tensile in the weld zone while the balancing compressive stress in HAZ at all rotational speeds (254 rpm to 870 rpm) and at all welding speeds (85mm/min to 185 mm/min).

Majority of the FEAs on FSW have emphasized on the study on the thermal distribution, peak temperature, shear stresses, residual stresses, thermomechanical behavior and force. Besides that, there are few researches investigate the flow of the material at the weld area. In conclusion, the FEAs do not possess the capability to study the other

mechanical properties such as tensile strength, grains size development, fatigue and etc. However, FEAs has the ability to simulate stress, temperature and flow of materials better than experimental investigation. Therefore, the researchers can leverage on these advantages of FEA and find the relationship of the parameters simulated in FEAs to enhance their researches.

2.2 Various FEA Modelling Methods on FSW Process

FEA modelling on FSW process is very complex. It is a complicated procedure that involves the interaction of thermal and mechanical phenomena. The rotational motion of the tools against the surface of the workpiece induces heat due to friction. The kinetic energy from the tool is converted into heat energy which is then being partially transferred to the workpiece. The process has caused excessive deformation and plastic straining. Due to these conditions, unique methods have been developed to elucidate the FSW process. The created methods need to be validated via experimental results and appropriate mathematical models. The discovered methods have been classified under three categories; thermal model, thermo-mechanical flow-based model, and thermal-mechanical non-flow based model (Iordache, Badulescu, Iacomì, Nitu, & Ciuca, 2016).

The thermal model is the simplest method to replicate the FSW Process. The model considered the tool as moving heat source because the main purpose of the tools is to generate heat. The method is able to avoid the huge element distortions caused by the penetration of tool in the workpiece. However, it has low accuracy especially on predicting stress-related parameters as it neglects the effect of tool motions.

In the flow-based model, the workpiece is model using traditional Lagrangian elements which become highly distorted during the simulation of FSW process. It may result in loss of accuracy of the FEA analysis. Several modelling techniques have been deployed to overcome the problem; Adaptive Remeshing and Arbitrary Lagrangian Eulerian (ALE). Flow-based models is developed using computational fluid dynamics (CFD). However, it has major limitations on inclusion of material hardening as it is only able to

elucidate rigid-viscoplastic material behavior (Iordache et al., 2016). Despite CFD, flow-based model can also be constructed using Coupled Eulerian Lagrangian method. It combines both Eulerian and Lagrangian approaches; the tool is developed as rigid isothermal Lagrangian body and the workpiece is developed using Eulerian formulation (Buffa et al., 2009). The interaction behavior between the tool and workpiece is defined as contact.

2.3 Finite Element Analysis (FEA) Softwares

There are 3 prominent softwares available in the market that have been used to develop Finite Element Modelling (FEM); ANSYS, FLUENT AND ABAQUS. These softwares have unique capabilities to perform FEM and the users need to be aware of the advantages and disadvantages of them.

FEMs are able to simulate the bending or twisting of the structures. They also can visualize the thermal distributions, stress distributions and displacement. According to Meyghani, Awang, Emamian, Mohd Nor, and Pedapati (2017), ABAQUS and ANSYS are the best option to perform the simulations and analysis on mechanical properties, deformation, heat transfers and temperature distributions. Kiral et al. (2013) have used ANSYS software to simulate the temperature distribution in the welded aluminium plate in the FSW process. Besides that, Yu, Zheng, and Lai (2018) has utilized ABAQUS software to investigate the temperature evolution during the plunge, dwell and moving stages of a friction stir welded 7050 aluminium alloy and the effect of heat conduction by the back plate. Meanwhile, FLUENT is the most suitable software to perform material flow and the fluid dynamic modelling. A research conducted by Hasan (2019) has applied FLUENT software to model the flash formation phenomena that occur during FSW process by using the volume of fluid method.

The study on FSW requires various aspects of analysis including thermomechanical behavior, fatigue behavior, plastic deformation, stress, friction modelling and the flow of materials. FLUENT and ANSYS are the appropriate softwares for the analysis. However, ABAQUS is the most suitable as it is supported with huge materials data and able to perform material flow analysis.

2.4 Properties of Aluminium Alloy, AA5083

The Aluminium-Magnesium alloy 5083 (AA5083) contains 4-4.9 wt% Mg and has undergoes strain hardening process. It is categorized under medium-strength, non-heat treatable wrought aluminium alloy and its strength can be increased by addition of Magnesium (Mg). It has advantages in term of economy of fabrication, weldability and corrosion resistance. It is supersaturated at room temperature as it contains more than 3 wt% Mg; the excess Mg solute atoms tend to precipitate out as β -phase (Mg_2Al_3) particles to the grain boundaries during continuous aging at room temperature or after short exposure to slightly elevated temperatures in the range of 65-200 °C; thus making it stronger and suitable for the application at room temperature. The melting point is at 570°C.

Table 2.1 shows the chemical compositions of AA5083 and AA6161 obtained from Summers et al. (2015).

Table 2.1 The chemical compositions of AA5083 and AA6061

Alloy	Si	Fe	Cu	Mn	Mg	Cr	Zn	Ti	Al
5083-H116	0.11	0.24	0.06	0.57	4.4	0.09	0.02	0.02	bal
6061-T651	0.66	0.4	0.24	0.07	0.9	0.18	0.02	0.02	bal

Table 2.2 shows the properties of AA5083 at different temperature obtained from Gupta, Llyod, and Court (2001) meanwhile Table 2.4-3 shows the mechanical properties of AA5083 at various temperatures extracted from Summers et al. (2015). As stated in the table, the mechanical properties and density decrease over time.

Table 2.2 The temperature dependent properties of AA5083

The material temperature dependent properties of AA5083.

Temperature (°C)	Conductivity (W/m °C)	Specific heat (J/Kg °C)	Density (Kg/m ³)
-20	112.5	924.1	2673.9
80	122.7	984.2	2642.7
180	131.6	1039.6	2629.4
280	142.3	1081.2	2611.5
380	152.5	1136.6	2589.3
480	159.5	1178.2	2567
580	177.2	1261.4	2549.2

Table 2.3 The temperature dependent mechanical properties of AA5083

Temperature dependent mechanical properties of AA5083.

Temperature [°C]	Young's modulus [GPa]	Poisson's ratio
25	72	0.33
100	70	
150	67	
200	62	
250	42	
300	41	
400	28	
500	15	

Figure 2.1 shows the strain-stress diagram of AA5083 at different temperatures extracted from Summers et al. (2015). It shows that the tensile strength of AA5083 is maximum at room temperature and it degrades as the temperature increases.

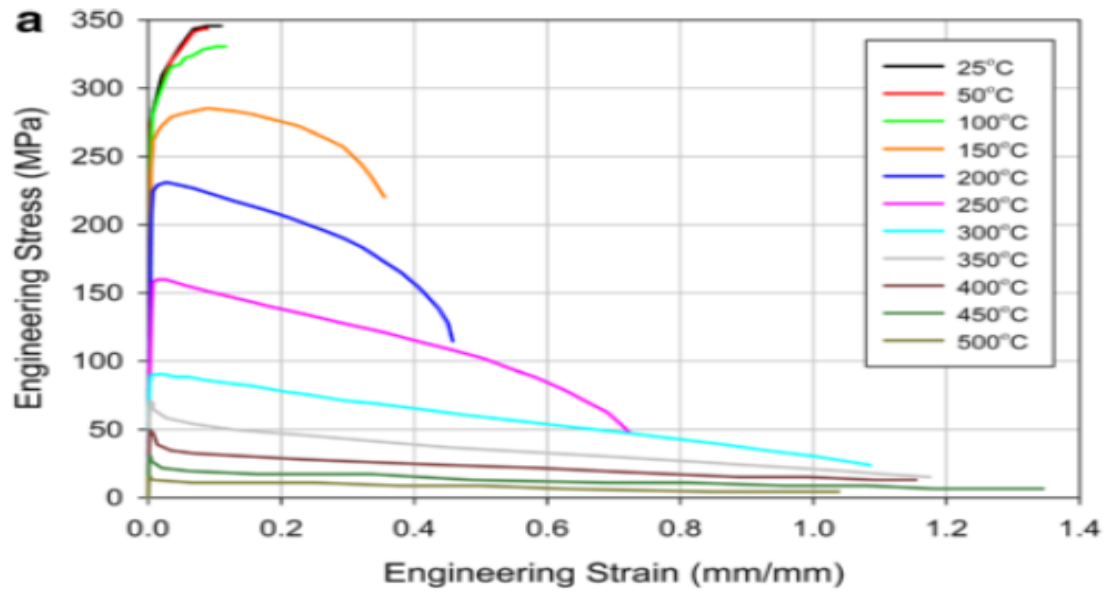


Figure 2.1 The strain-stress diagram of AA5083 at different temperature

2.5 Johnson Cook Material Model

The model has been widely used in finite element analysis. It is suitable to predict the first-order metal-metal working effects such as rate of deformation and the attendant temperature which normally occurs in plastic deformation of metallic materials. It assumes the material as isotropic linear-elastic and a strain-rate sensitive, strain-hardenable and thermal softenable plastic (reversible)(Gambirasio & Rizzi, 2014). The elastic mechanical properties are purely defined by generalized Hooke's law. Whereas, the elastic-plastics characteristics is described based on yield criterion, flow-rule and constitutive law. Yield criterion is a mathematical model that describes the conditions for the creation and continuation of plastic deformation; the flow rule relates the rate of change of different plastic strain components; the constitutive law relates the changes in material-strength with the plastic deformation, temperature and rate of deformation.

According to Grujicic, Pandurangan, Cheeseman , and Yen (2011), FSW process causes plastic deformation of the workpiece that is assumed to be purely distortional (non-volumetric). Von Misses yield describes the yield criterion as the equivalent stress of scalar, frame-invariant function of stress components needs to be equal or greater than the yield stress of the material to undergoes plastic deformation. The normality flow rule is applied in the FEA analysis to describe the plastic flow of the material to follow the direction of stress-gradient of the yield surface. Johnson-Cook strength constitutive law states an equation as below:

$$\sigma_y = A \left[1 + \frac{B}{A} (\varepsilon^{-pl})^n \right] \left[1 + C \log(\varepsilon^{-pl} / \varepsilon_0^{-pl}) \right] [1 - T_H^m] \quad (1)$$

Where,

ε^{-pl} : Equivalent plastic strain rate ε_0^{-pl} : Reference equivalent plastic strain rate

A : Zero-plastic strain, unit plastic-strain rate, room-temperature yield strength

B : Strain-hardening constant

m : Thermal-softening exponent

$$T_H = (T - T_{room}) / (T_{melt} - T_{room})$$

Based on the eq. 1, term A is the yield stress of the as-annealed material which has been considered as constant in a value. The first pair of bracket describes the effect of strain hardening; the second pair of bracket defines the deformation rate effects; the last pair of bracket quantifies the reversible effect of temperature.

The table 2.4 shows the parameters of Johnson-Cook Model for Aluminium Alloy, AA5083 which has been extracted from the report published by Rashed, Yazdani, Babaluo, and Hajizadeh Parvin (2016).

Table 2.4 Johnson Cook Model Paramters for Aluminium Alloy, AA5083

Parameter	Symbol (unit)	Value		
		Aluminum	Steel	Tungsten alloy
Johnson–Cook model				
Density	R_o (kg/m ³)	2700	7860	17,600
Shear modulus	G (Pa)	2.69×10^{10}	8.18×10^{10}	160×10^9
Elastic modulus	E (Pa)	70×10^9	20.9×10^{10}	–
Poisson's ratio	PR	0.3	0.28	–
Yield stress	A (Pa)	1.67×10^8	7.92×10^8	1.506×10^9
Hardening constant	B (Pa)	5.96×10^8	5.1×10^8	177×10^6
Strain rate constant	C	0.001	0.014	0.016
Thermal softening exponent	M	0.859	1.03	1
Hardening exponent	N	0.551	0.26	0.12
Melting temperature	TM (K)	893	1790	1723
Room temperature	TR (K)	300	300	300
Ref. strain rate	$EPSO$ (s ⁻¹)	1	1	1
Specific heat	CP (Jkg ⁻¹ K ⁻¹)	910	477	134
Pressure cutoff	PC (Pa)	-1.5×10^9	–	–
Failure parameter	$D1$	0.0261	0.05	0
Failure parameter	$D2$	0.263	3.44	0.33
Failure parameter	$D3$	–0.349	–2.12	–1.5
Failure parameter	$D4$	0.247	0.002	0
Failure parameter	$D5$	16.8	0.61	0
Add_erosion model				
Max. effective strain at failure	$EFFEPS$	2	2.1	1.5
EOS ⁵ linear polynomial				
Bulk modulus	CI (Pa)	5.83×10^{10}	1.59×10^{11}	310×10^9

CHAPTER 3

METHODOLOGY

3.1 FE Modelling Using Coupled Eulerian Lagrangian Method

1. Constructing Geometry Model

The FSW modelling was developed using Coupled Eulerian-Lagrangian Method. It involved constructing workpiece model with 2 plates; Euler Plate and Reference Plate. Meanwhile, the tool was constructed as Lagrangian model. Euler model was used in the workpiece model as it able to deal with high deformation. The method assumed the euler model would flow through the Lagrangian model. The reference plate was 3D deformable extruded while the Euler Plate was Euler model; both with dimensions of 60 x 40 x 5 mm. The tool had pin with radius of 2.4 mm with length of 3.5 mm, and shoulder radius of 5.1 mm. The heat energy was generated from the friction between the tool shoulder and plate as the tool rotated.

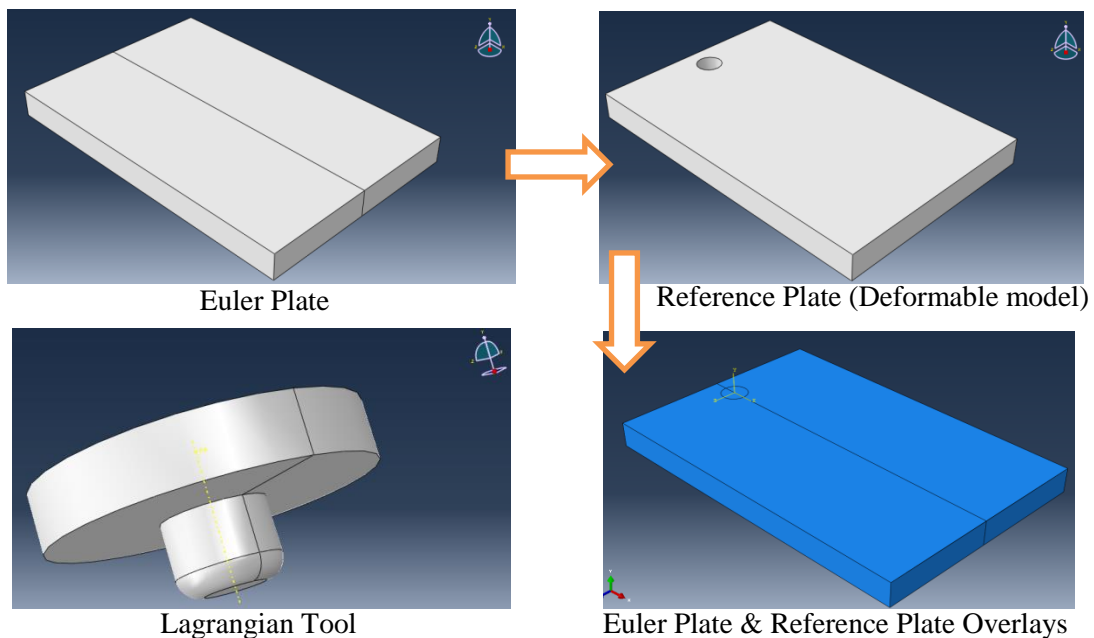


Figure 3.1 The Model of Euler Plate, Reference Plate & Tool

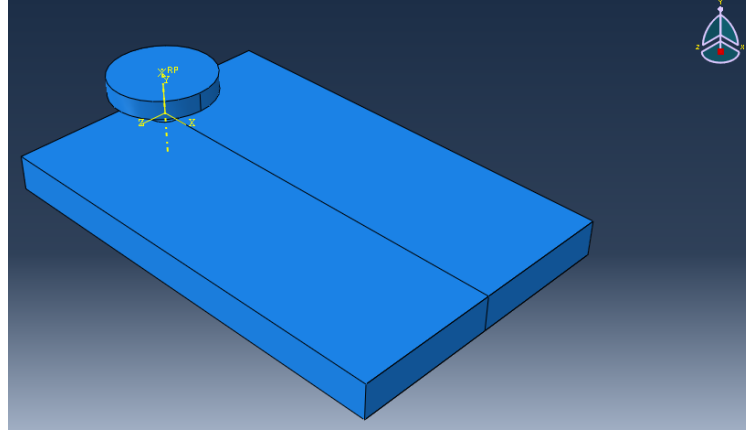


Figure 3.1 The Assembly of the Models

Besides that, the model dimensions and other measurable properties such as specific heat capacity, pressure, stress and strain need to adhere to a specific set of units. It was due to Abaqus software did not have any specific units. Any value applied in the modelling had no unit. Thus, the users needed to set the units used in the modelling based on the table 3.1 which was extracted from Iordache et al., (2016). It was to maintain the unit consistency. In this project, the modelling was constructed by using SI(mm) units.

Table 3.1 The Set of Unit Used in Abaqus

Quantity	SI	SI(mm)	SI	US Unit(ft)	US Unit(inch)
Length	<i>m</i>	<i>mm</i>	<i>m</i>	<i>ft</i>	<i>in</i>
Force	<i>N</i>	<i>N</i>	<i>kN</i>	<i>lbf</i>	<i>lbf</i>
Mass	<i>kg</i>	<i>tonne (10³kg)</i>	<i>tonne</i>	<i>slug</i>	<i>lbf s²/in</i>
Time	<i>s</i>	<i>s</i>	<i>s</i>	<i>s</i>	<i>s</i>
Stress	<i>Pa (N/m²)</i>	<i>MPa (N/mm²)</i>	<i>kPa</i>	<i>lbf / ft²</i>	<i>psi (lbf / in²)</i>
Energy	<i>J</i>	<i>mJ (10⁻³J)</i>	<i>KJ</i>	<i>ftlbf</i>	<i>inlbf</i>
Density	<i>kg/m³</i>	<i>tonne/mm³</i>	<i>tonne/m³</i>	<i>slug/ ft³</i>	<i>lbf s²/in⁴</i>

2. Generates Mesh

The Euler Plate model and Tool model were meshed with element size of 1 mm. Meanwhile, the Reference Plate model remained unmeshed. The thermos-mechanical model was assigned as EC3D8RT element, an 8-node thermally coupled linear eulerian brick, reduced integration, hourglass control. For the tool, it was assigned as C3D8RT element, an 8-node thermally coupled brick, trilinear displacement and temperature, reduced integration, hourglass control. The Euler Plate would had a total of 12 000 elements.

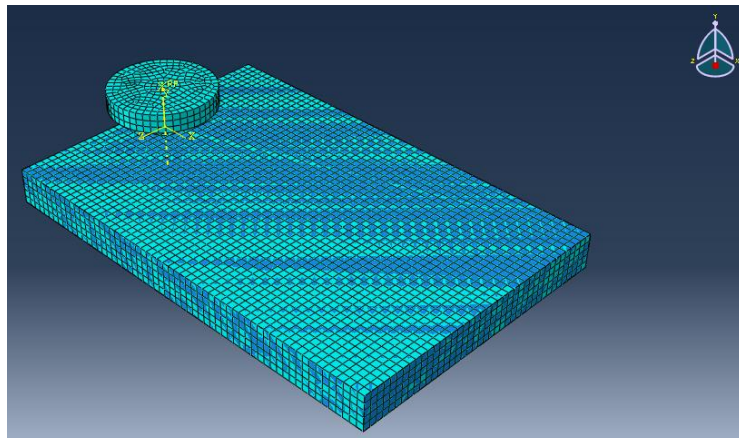


Figure 3.3 Meshed Euler Plate and Tool

3. Determines the Boundary Conditions

The Euler Plate was completely fixed at both sides of the plate while the remaining surface had 6 degree of freedom (DoF). The tool model was a rigid body with its center as the reference point. The reference point had restricted motion of rotation about y-axis and translation along x-axis only; the rest of the motion had been fixed. These boundary conditions were based on the real situation during the FSW process.

4. Determines Welding Process Parameters.

Table 3.2 represented the relationship of Tool rotational speed (TRS), Tool Speed (TS), Tool Tilt Angle (TTA) with the mechanical properties of AA5083 obtained from Kundu and Singh (2017). According to their research, they found that FSW on AA5083 with rotational speed of 950 rpm, welding speed of 28 mm/min and tilt angle of 3° have the highest Ultimate Tensile Strength (UTS) of 315 MPa which is slightly lower than the UTS of AA5083 at room temperature. Translational speed of 28 mm/min would produce the highest UTS for every rotational speed. However in this study, tool rotational speed had been fixed at 500 rpm with varying translation/transverse speed. The steel-H13 type of tool that consists of flat shoulder – 14 mm diameter and tool pin – 4.8 mm diameter and 3.5 mm length would be used. The tool penetration depth was fixed at 3.5 mm from the upper touch point. The plate was heated up to its recrystallization temperature which $1/3$ of the melting temperature of AA5083.

Table 3.2 The relationship of Tool rotational speed (TRS), Tool Speed (TS), Tool Tilt Angle (TTA) with the mechanical properties of AA5083

Ex. no.	Input process parameters			Responses (avg.)		
	TRS (r/min)	TS (mm/min)	TTA ($^{\circ}$)	UTS (MPa)	% EL	Micro-hardness (HV)
1	500	16	1	232	2.75	69
2	500	28	2	298	3.10	71
3	500	40	3	257	3.70	73

5. Load Calculation

The model was subjected to surface heat flux thermal load as the rotational motion of the tool shoulder against the surface of the workpiece induces frictional heat. Besides that, the tool pin also contributed to the heat energy generated. According to M. M. El-Sayed et al. (2018), the surface heat flux varied with the step time as the amount of load decreasing over the step time. The reason is the shoulder-workpiece interface becomes softer as the step time increase. The surface heat flux (Q) is calculated by using the following equations:

$$\text{Heat Flux } (Q) = \frac{\text{Heat input } (q)}{\text{Area } (A)} \text{ (w/m}^2\text{)} \quad (2)$$

Where, the heat input (q) is calculated by Frigaard, Grong, and Midling (2001) as follows:

$$\text{Heat input } (q) = \int_0^R 2\pi\mu\omega Pr^2 dr \text{ (w)} \quad (3)$$

$$\omega = \frac{2\pi n}{60} \quad \text{By substituting in (3)}$$

$$q = \int_0^R \frac{2}{30} \pi^2 \mu P n r^2 dr \quad (4)$$

$$q = \frac{1}{45} \pi^2 \mu P n (R^3 - r^3) \text{ (w)} \quad (5)$$

where:

ω : Angular velocity (rad/sec)

n : Rotational speed (rpm)

P : Pressure, $P = \frac{F}{A}$ (MPa)

A : Area, $n = \pi(R - r)^2$ (mm²)

The following assumptions have been made to perform the calculation:

- Friction coefficient, $\mu = 0.3$
- Axial Force, $F = 5000 \text{ N}$
- Shoulder radius, $R = 5.1 \text{ mm}$
- Pin radius, $r = 2.4 \text{ mm}$
- Rotational speed, $n = 500 \text{ rpm}$
- The heat loss via convection and radiation from the plate surfaces to the surrounding are neglected.
- The heat loss through conduction between the bottom surface of the plate and the backing plate are also ignored.
- Only 50% of the heat energy produced has been absorbed by the workpiece.

Based on the calculation using the eq. 2, the heat flux and heat energy per time (power) for the given conditions are as follows:

$$Q (500 \text{ rpm}) = 1659516.575 \text{ W/m}^2 \qquad q (500 \text{ rpm}) = 510.977593 \text{ W}$$

The heat flux movement along the welding line is at constant speed and it is governed by the following equation:

$$Z_{i+1} = Z_i + V_t \Delta t \qquad (6)$$

where:

Δt : The time required for the tool to travel from location Z_i to Z_{i+1} (i.e. element size)

V_t : The tool travel speed

The heat transfer between the tools and work piece is governed by the Fourier law of heat conduction that has been used in Kiral et al. (2013) as below:

$$\rho C_p \frac{\partial T}{\partial t} = \frac{\partial}{\partial x} \left(K_x \frac{\partial T}{\partial x} \right) + \frac{\partial}{\partial y} \left(K_y \frac{\partial T}{\partial y} \right) + \frac{\partial}{\partial z} \left(K_z \frac{\partial T}{\partial z} \right) \quad (7)$$

where:

- K : The heat conductivity
- C_p : The specific heat
- T : Temperature
- ρ : Density
- t : The time x, y, z : The spartial coordinates

6. Performing the Simulation and Capturing the Results

Several simulations had been conducted to study the effect of difference welding speed on the thermal induces stress. The other process parameters had been fixed as has been mentioned earlier. The generated result from the simulation will be tabulated in a table for analysis and comparison. The graphical results had been captured for the purpose of analysis.

7. Results Validation

The results produced by the simulations need to be validated before further analysis are conducted. It is conducted by comparing the results of simulation with the theoretical logics, others researches results and values from theoretical calculation. In term of theoretical logics, the biggest residual stresses developed at the regions where the temperature differences are the highest. In FSW, the biggest temperature differences occur at the regions in contact with the edges of the tool. Besides that, the temperature distribution must be initiated at the sources and dispersed and cooled away overtime. The temperature generated from the friction must be able to soften the material. Furthermore, there is no deformation on the model because it is supported in all directions.

Despite of comparing the results with the previous researches, the results also have been compared with the theoretical calculation on the important regions. The calculation is basically on the temperatures developed on the model during the process. The formulas used in the theoretical calculation are as given in the load calculation earlier.

8. Analysis of Results

The validated results of the simulation have been analyzed to determine the best welding speed for a fixed process parameters and conditions. The tables that contained results of temperatures and residual stresses at every node according to various welding speeds are examined to determine the best welding speed.

3.2 Time Scaling Approach

FEA analysis on FSW process required long time to be completed. As it was very time consuming analysis, the practicality of numerical approaches to study the process has become arguable. It was due to the time needed to complete the numerical analysis was too long to be compensated with its economic advantages. It was attributed to the high deformation that occurs throughout the process as the tool plunged into the workpiece as it was softened by the heat generated due to friction. In FEA, it was necessary to apply explicit method of analysis instead of implicit method for high deformation simulation. This method was highly accurate but it was a time consuming analysis compare to implicit method. Therefore, time-scaling was very important if possible to significantly reduce the time needed to complete the analysis.

The idea of the approach was to speed up the simulated process while maintaining the rate of heat transfer between tool and workpiece. There were two main process parameters that controlled the heat generated; welding transverse speed and rotational speed. Besides that, reducing the simulation time required the increase of heat energy generated to maintain the same rate of heat transfer which could be achieved through increasing of transverse speed and rotational speed. The following formula was used to govern the amount of heat energy generated, q :

$$q = \frac{1}{45} \pi^2 \mu P n (R^3 - r^3) \quad (5)$$

Based on the formula, the rotational speed, n was the only variable parameter and the remaining parameters were kept constant. Therefore, we could deduce that the amount of heat generated was directly proportional to the rotational speed.

Meanwhile, transverse speed had an important role in heat transfer between the tool and workpiece. Heat transfer was governed by the following equation:

$$q = mc_p\theta \quad \Longrightarrow \quad q = VA\rho c_p\theta \quad (8)$$

V : Transverse speed

A : Area

c_p : Specific heat capacity

θ : Changes in temperature

Based on the equation, the term of interest was changes in temperature θ ,. By rearranging the formula, it was found that the changes in temperature should be linear correlated with welding speed. Based on these findings, there was possibility to apply time-scaling in the numerical analysis of FSW process.

The increment of the transverse speed and rotational speed should be fixed by a certain ratio which primarily depended on the time required to complete the welding of a specific distance (length of workpiece).

Table 3.3 Welding Transverse Speed and Rotational Speed Before Time-Scaling

Before time-scaling					
TS, (mm/min)	TS, (mm/s)	TRS, (RPM)	TRS, (rad/s)	WP length, (mm)	Time required, (s)
16	0.266666667	500	52.35987756	20	75
28	0.466666667	500	52.35987756	20	42.85714286
40	0.666666667	500	52.35987756	20	30
80	1.333333333	1000	104.7197551	20	15

Table 3.4 Welding Transverse Speed and Rotational Speed After Time-Scaling

After time-scaling			
Planned time required, (s)	Scaling factor	TS*, (mm/s)	TRS*, (rad/s)
1	75	20	3926.990817
1	42.85714286	20	2243.994753
1	30	20	1570.796327
1	15	20	1570.796327

Note: TS: Transverse Speed; TRS: Tool Rotational Speed; WP: Workpiece.

List of equations used to derive the values in table 3.2-1 and table 3.2-2 were as follows:

$$Time\ required = WP\ length / TS \quad (9)$$

$$Scaling\ factor = \frac{Time\ required}{Planned\ Time\ Required} \quad (10)$$

$$TS^* = TS \times scaling\ factor \quad (11)$$

$$TRS^* = TRS \times scaling\ factor \quad (12)$$

Besides that, the mechanical properties of aluminum alloy, AA5083 were believed to be not affected by the time-scaling approach. Some of the mechanical properties included in the FEA modelling in this study were specific heat capacity, thermal conductivity, density and elasticity. These properties were temperature-dependent properties. As the temperature of the workpiece in the process was depended on the rate of heat transfer, these properties should not cause significant problem to implement time-scaling in the analysis. If there was any problem, the effect should be minimal as the relationships of these properties with temperature were almost linear except for elasticity.

The relationship of specific heat capacity of AA5083 with temperature was near linear as shown as in figure 3.4.

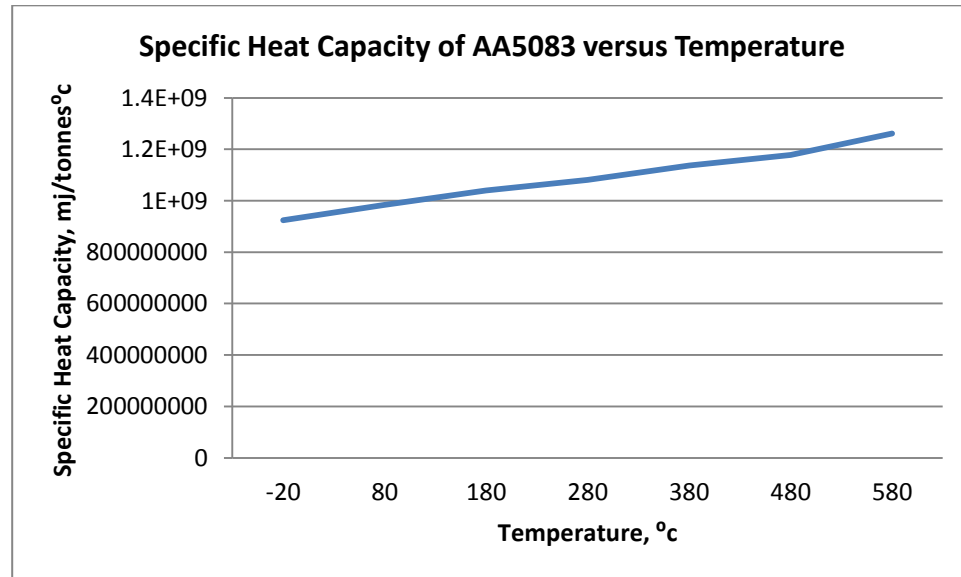


Figure 3.4 Relationship of Specific Heat Capacity of AA5083 and Temperature

The relationship of thermal conductivity of AA5083 with temperature was almost linear as shown as in figure 3.5.

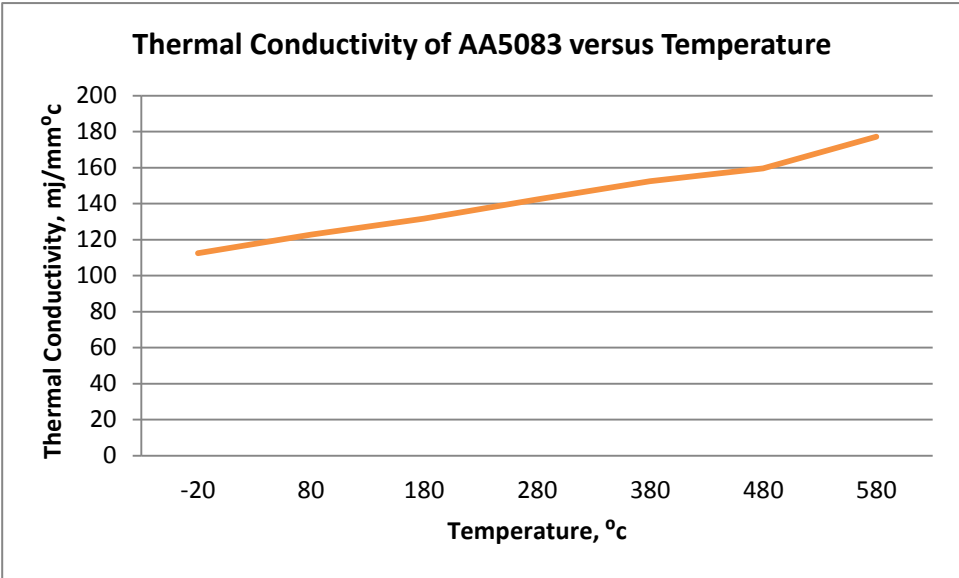


Figure 3.5 Relationship of Thermal Conductivity of AA5083 and Temperature

The relationship of density of AA5083 with temperature was nearly proportional as shown as in figure 3.6.

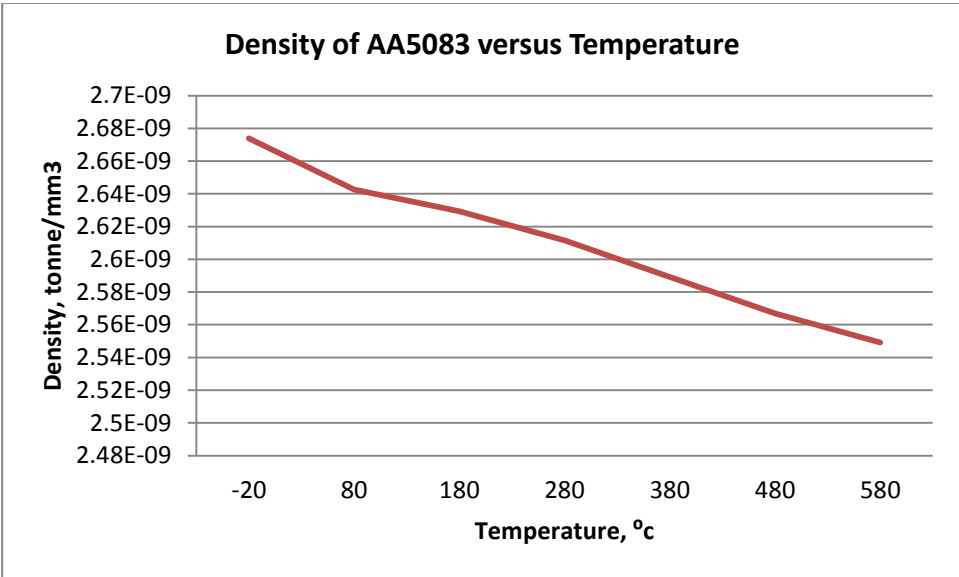


Figure 3.6 Relationship of Density of AA5083 and Temperature

However, the relationship of elasticity of AA5083 with temperature was not linear as shown as in figure 3.7. This would require further FEA analysis (not included in these study) on stress and strain of AA5083 during the FSW process.

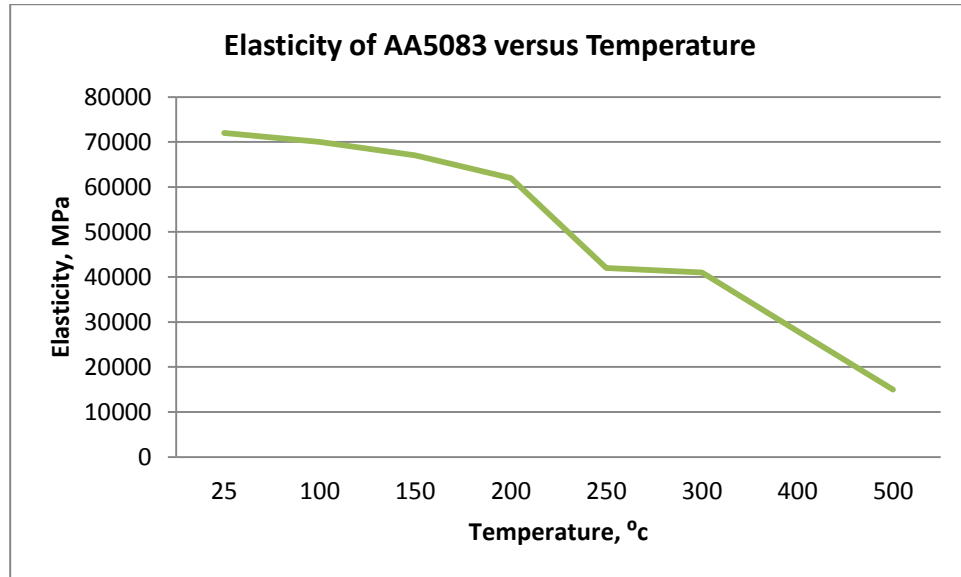


Figure 3.7 Relationship of Elasticity of AA5083 and Temperature

3.3 Project Activities / Gantt Chart

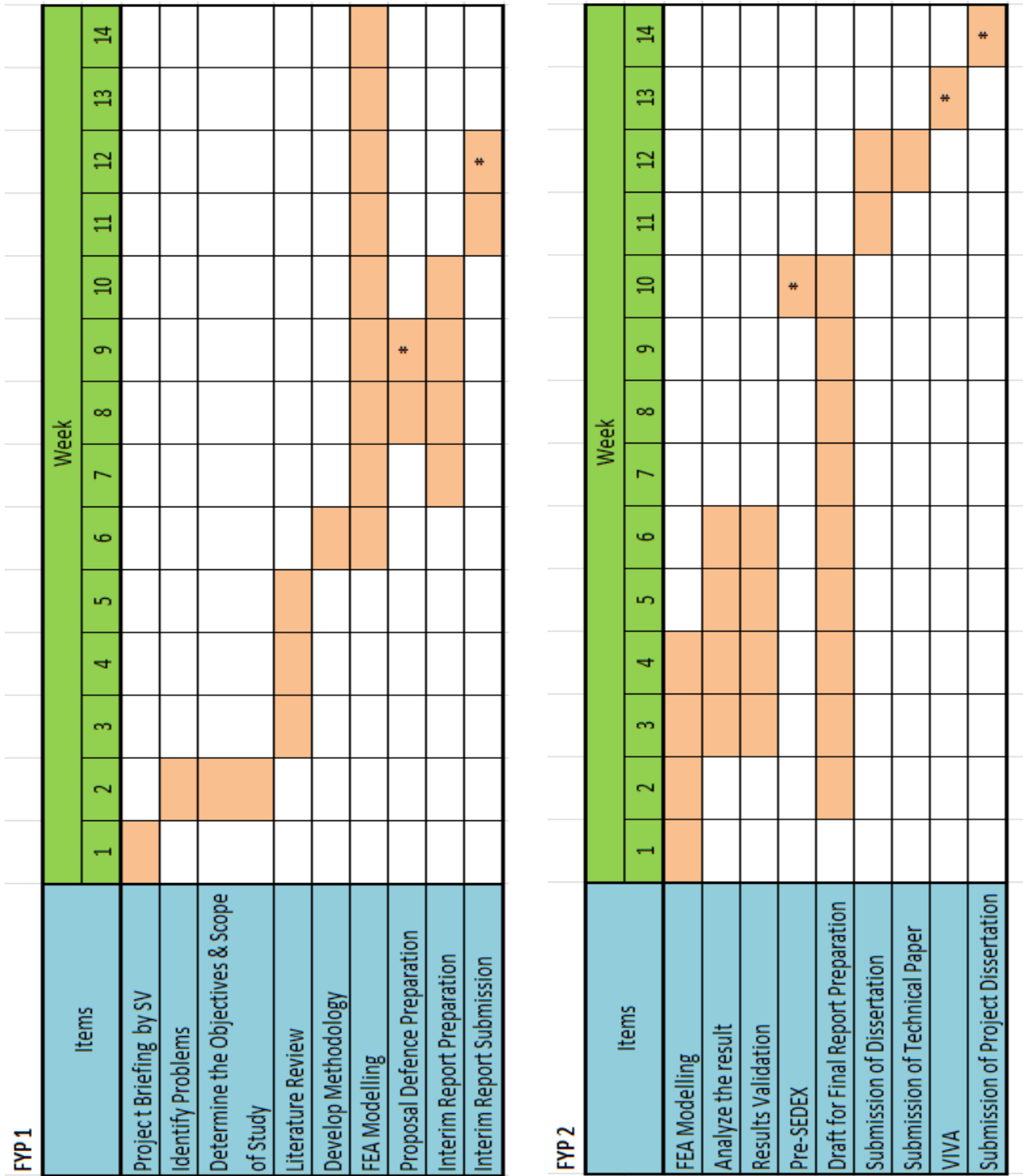


Figure 3.8 The gantt chart of the project

CHAPTER 4

RESULT AND DISCUSSION

4.1 Estimated Heat Energy and Temperature

The frictional energy produced by the rotation of the tool against the surface of the workpiece. Based on the conservation of energy theory, it was assumed that energy cannot be created and destroyed. Therefore, this study assumed that all the frictional energy was converted to heat energy. In the real condition of FSW process, not all the heat energy created being transferred to the workpiece. Some of the energy lose to surrounding and absorbed by the workpiece holder.

The theoretical calculations were used to validate the result of the FE simulation. The values in the table were derived by using the equation available in the methodology.

There are few assumptions made in the calculation:

1. The heat energy absorbed by the workpiece was 50% of the total energy created by friction. The remaining was assumed lose to the surrounding (air and workpiece holders).
2. The calculation of heat transfer between tool and workpiece was based on steady-state conditions. It was defined as the total heat energy absorbed by the workpiece throughout the FSW process was being used to increase the temperature of the workpiece as whole.
3. The pressure considered in the calculation was the result of force over the shoulder area.

Based on the table 4.1-1, the total amount of heat energy created based on the simulation with time-scaling method and the simulation without time-scaling method were similar. It was due to the lower heat energy created by lowering its processing time was compensated by increasing rotational speed. Thus, it proved that time-scaling method can be applied in FE simulation of FSW welding. The highest heat energy calculated when the welding speed was the lowest. It was expected that FE simulation with welding speed 16mm/min would have the highest temperature.

Table 4.1 Theoretical Calculation for Heat Energy Created & Temperature of the Workpiece Based on Steady-State Conditions

Status	Welding Speed, v (m/s)	Rotational speed, η (rpm)	Heat Input, q (w)	Time required for welding, s	Total Heat Energy, Q (J)	1/2 of Energy Transferred, (J)	Min. Final Temperature Expected, K	Min. Final Temperature Expected, °c
Simulation without TS	0.0002667	500.000	510.977593	74.99062617	38318.52966	19159.26483	861.3754164	588.2254164
Simulation without TS	0.0004667	500.000	510.977593	42.85408185	21897.47559	10948.7378	619.9974792	346.8474792
Simulation without TS	0.0006667	500.000	510.977593	29.99850007	15328.56136	7664.280681	523.4390634	250.2890634
Reference	0.0013334	1000.000	1021.955186	14.99925004	15328.56136	7664.280681	523.4390634	250.2890634
Simulation with TS	0.02	37500	38323.31947	1	38323.31947	19161.65974	861.4458233	588.2958233
Simulation with TS	0.02	21428.57143	21899.0397	1	21899.0397	10949.51985	620.0204705	346.8704705
Simulation with TS	0.02	15000	15329.32779	1	15329.32779	7664.663895	523.4503293	250.3003293

Constant	π	Friction Coefficient, μ	Axial Force, F (N)	Pressure, (Pa)	Shoulder Radius, R (m)	Pin Radius, r (m)	$R^3 - r^3$
Value	3.141592654	0.3	5000	16238643.31	0.0099	0.0024	9.56475E-07

Constant	WP Width, w (m)	WP Length, L (m)	WP Thickness, Th (m)	Initial Temp, To (°c)	WP Specific Heat Capacity, (Cp)	WP Thermal Conductivity, k (W/m.k)	WP Density	Welding Distance, m
Value	0.04	0.06	0.005	298.12	1086.471	205	2609	0.02

4.2 Graphical Result of FE Simulation for FSW Welding

The figure shows FE simulation of FSW welding by using Abaqus software. As mentioned in the methodology, the modelling was developed based on Coupled Eulerian-Lagrangian method. The tool rotated against the surface of workpiece which was then produced heat energy to increase the temperature and soften the workpiece along the welding line. The temperature distribution was graphically shown in the figures. As the workpiece was created as Eulerian material, the soften metal would flow as a fluid around the tool pin (Lagrangian body).

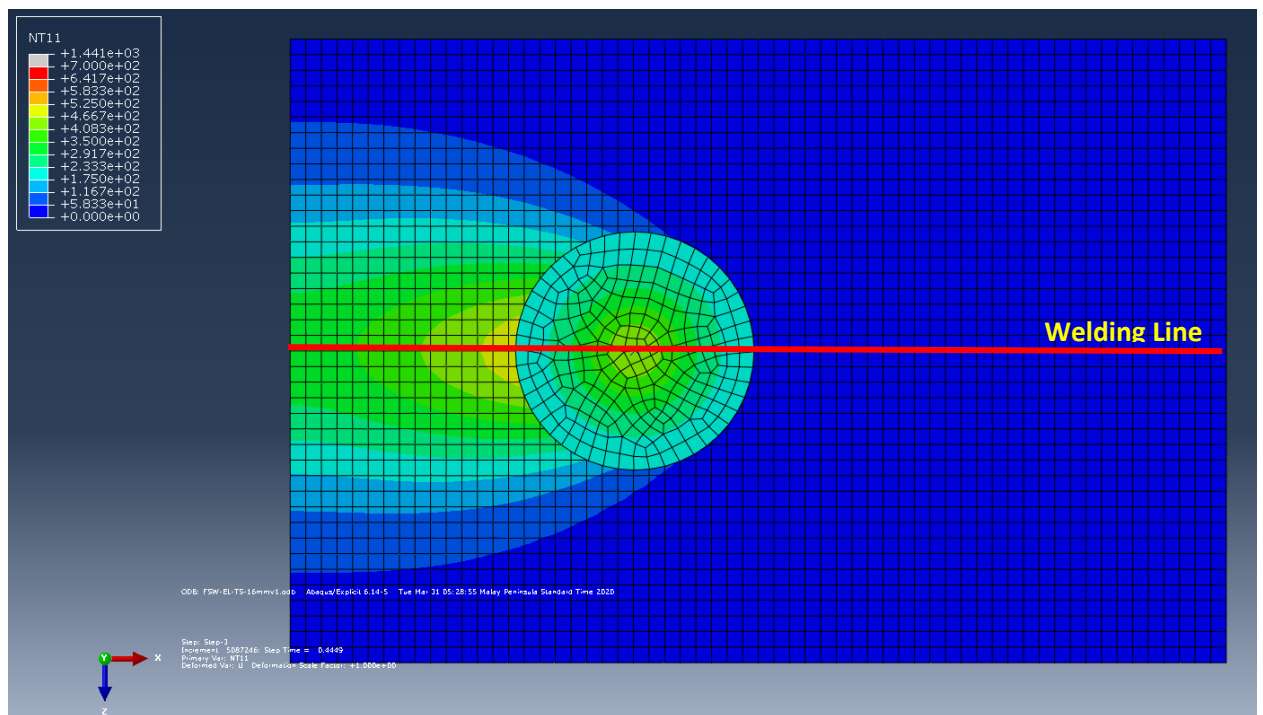


Figure 4.1 FSW with Time-Scaling (500 RPM, 16 mm/min)

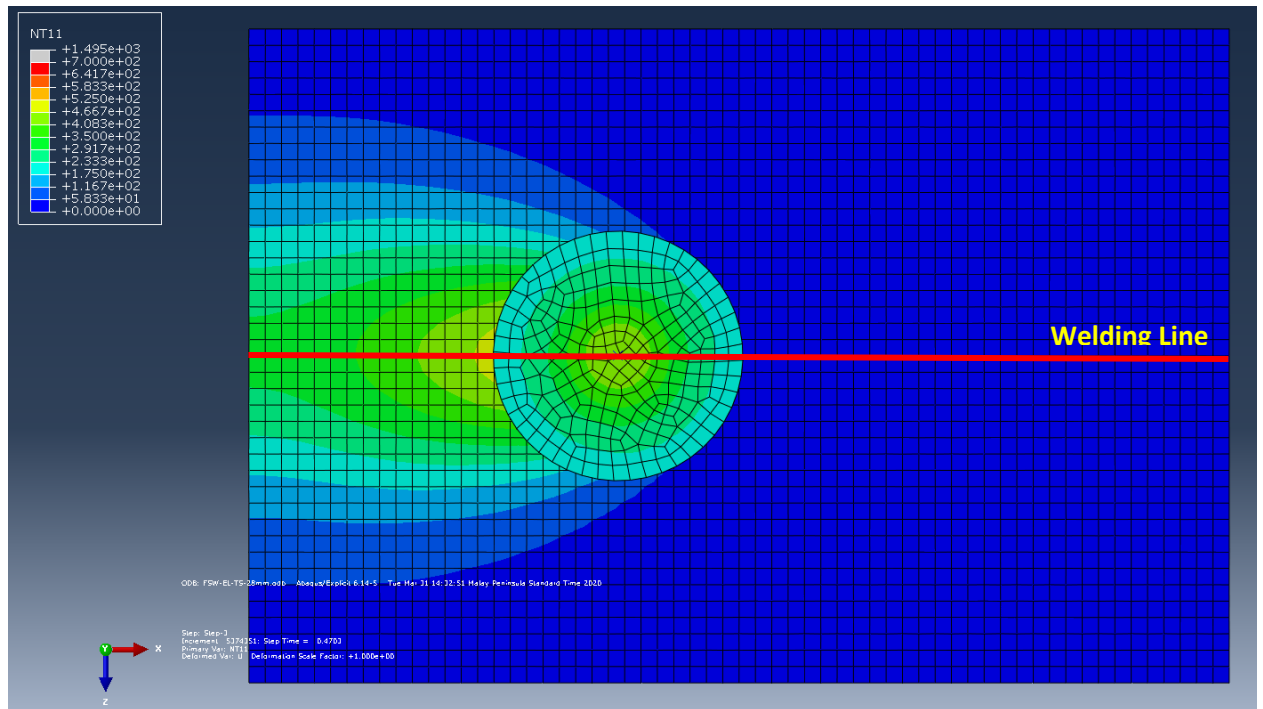


Figure 4.2 FSW with Time-Scaling (500 RPM, 28 mm/min)

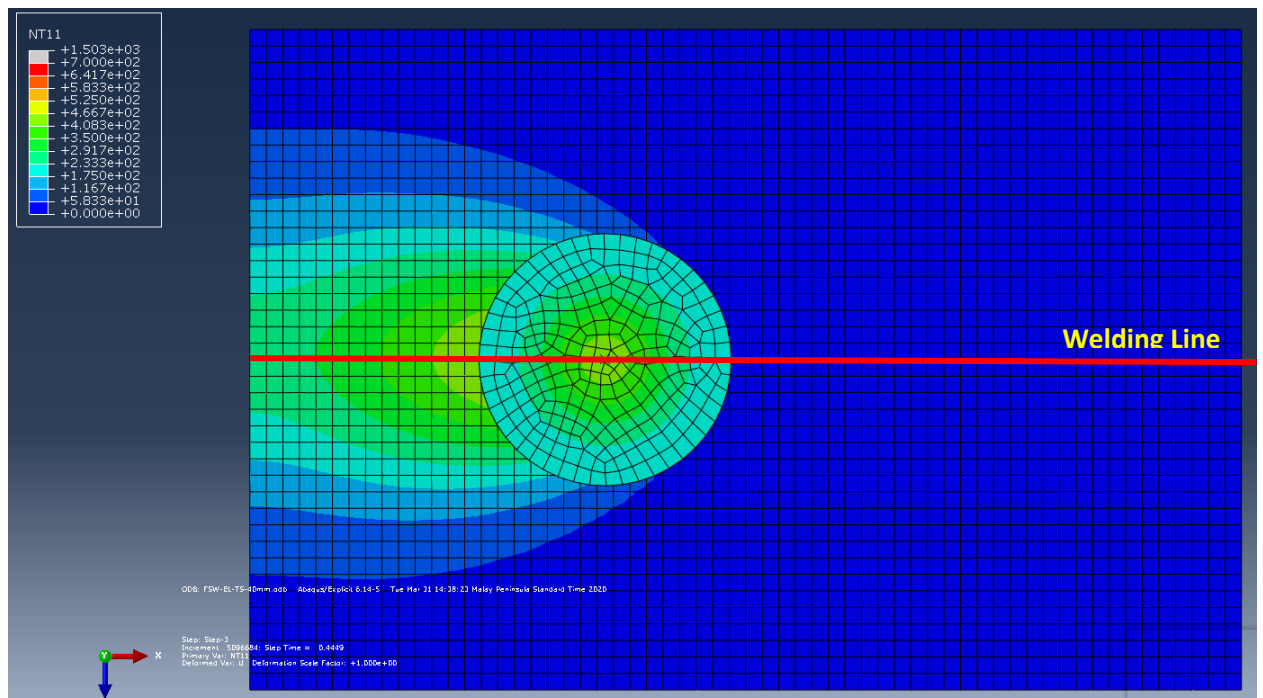


Figure 4.3 FSW with Time-Scaling (500 RPM, 40 mm/min)

4.3 Temperature Distribution along Z-axis

Temperature distribution was recorded to serve as the primary method to validate the accuracy of the modelling. The data was obtained by from the nodes placed on the line perpendicular to the welding line. The temperature was taken at four different zones; P1mm, P4mm, P8mm and P12mm. PXmm was the code used where X was the distance from the tool.

FSW Welding (500 rpm, 16 mm/min)

Based on the figure 4.4, the highest temperature recorded by FSW welding with rotational speed of 500 rpm and welding speed of 16mm/min was 501. 923°C. The temperature was recorded at near the tool pin. However, the temperature derived from the steady-state calculation was 588.22°C which was higher by 87.7°C and it was actually beyond the melting temperature of the aluminium alloy, AA5083. Besides that, it should be lower than the temperature obtained from the simulation as it implied the heat had been distributed evenly throughout the material. Therefore, the theoretical temperature calculated for the welding parameter was not valid as it supposed to include latent heat of fusion energy in the calculation. Meanwhile, the temperature obtained from the simulation was below the melting point of the material and could be accepted.

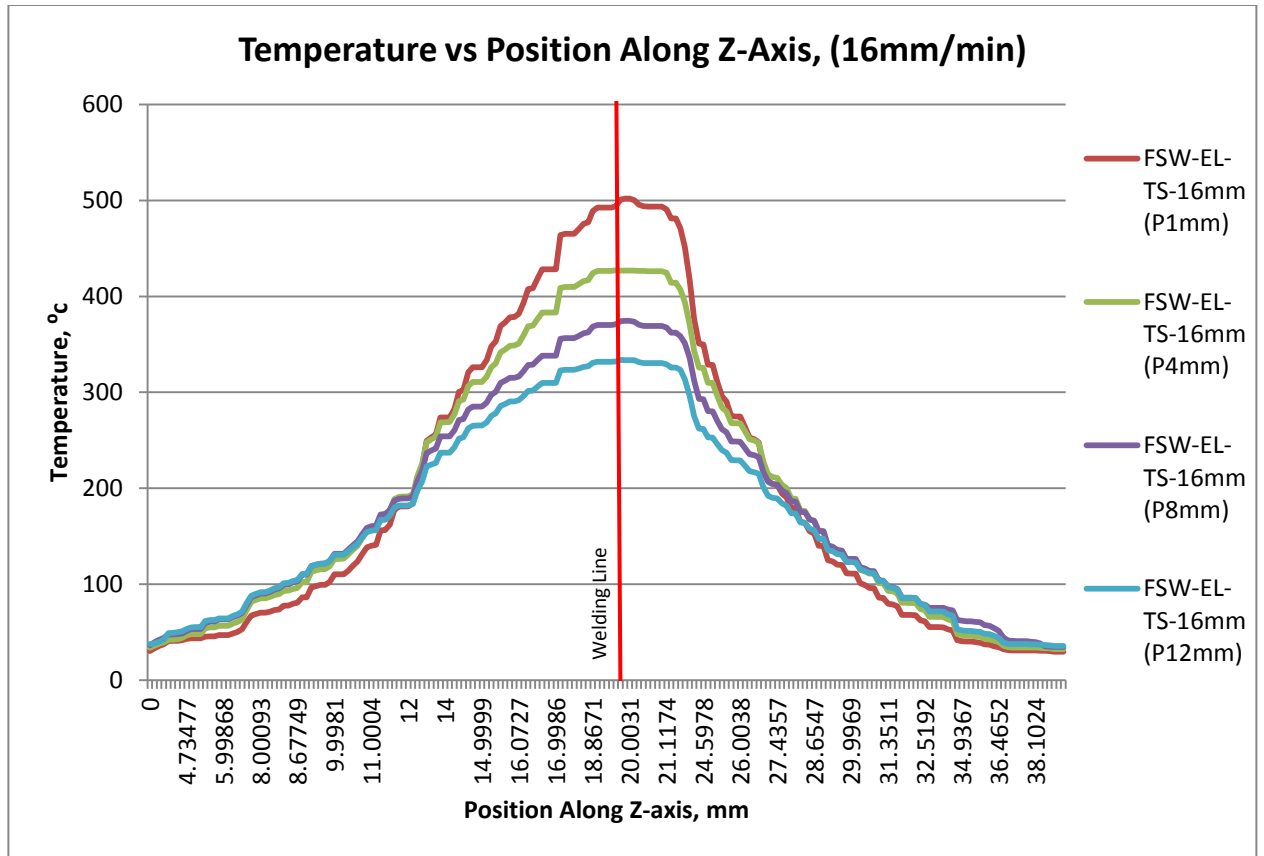


Figure 4.4 Temperature Distribution of FSW Welding (500 rpm, 16 mm/min)

FSW Welding (500 rpm, 28 mm/min)

According to the figure 4.5, the highest temperature obtained throughout the FSW process was 465.961⁰c. The temperature was also recorded near the tool pin. The theoretical temperature calculated based on steady-state behavior was 346.85⁰c; lower than temperature recorded in simulation by 119.11⁰c. It was about 34.34% higher than its steady-state value. This behavior was expected as the steady-state temperature was calculated with the assumption of the system was already in equilibrium state.

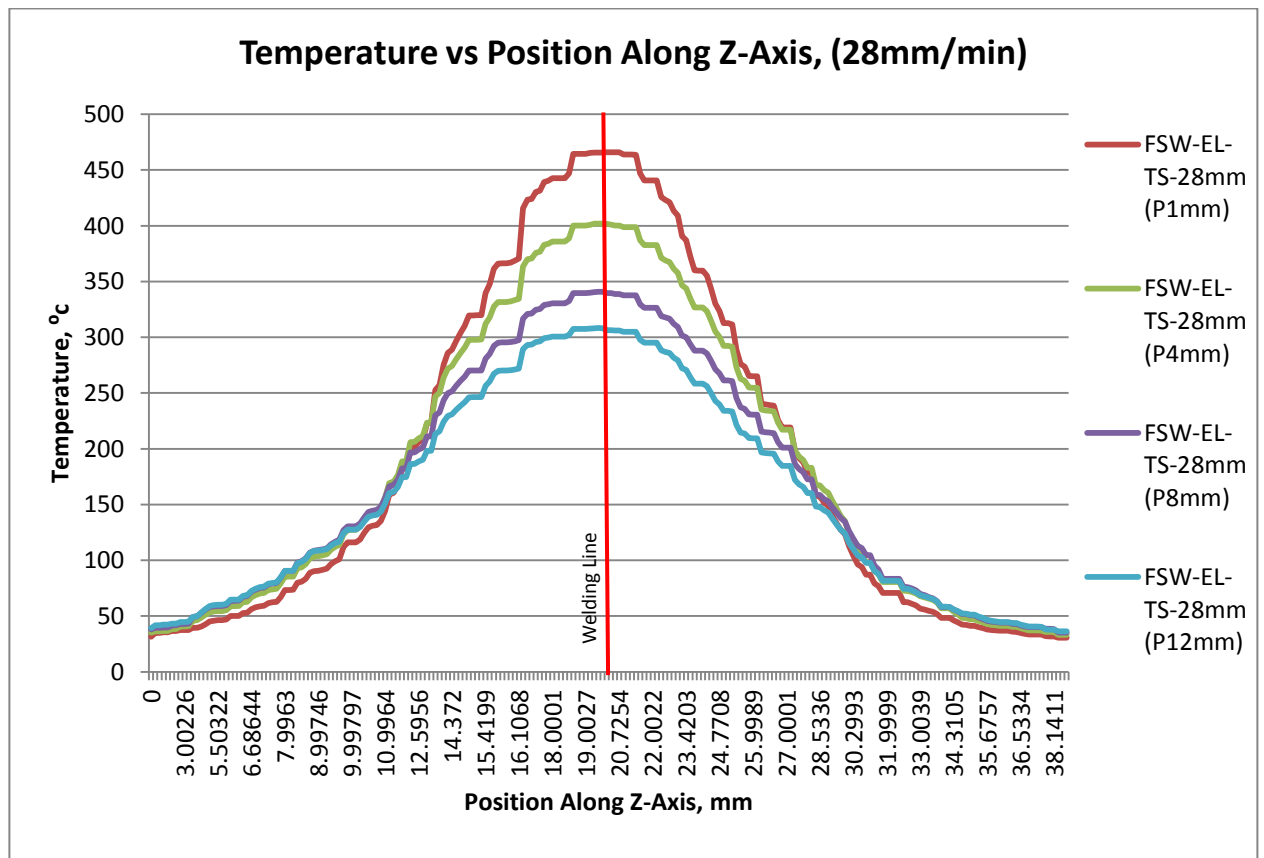


Figure 4.5 Temperature Distribution of FSW Welding (500 rpm, 28 mm/min)

FSW Welding (500 rpm, 40 mm/min)

Based on figure 4.6, the highest temperature obtained throughout the FSW process was 468.967°C . The temperature was also obtained close to the tool pin. The theoretical temperature calculated based on steady-state behavior was 250.29°C ; lower than temperature recorded in simulation by 218.677°C . It was about 87.37% higher than its steady-state value. This behavior was expected as the steady-state temperature was calculated with the assumption of the system was already in equilibrium state (same temperature for the whole of the workpiece).

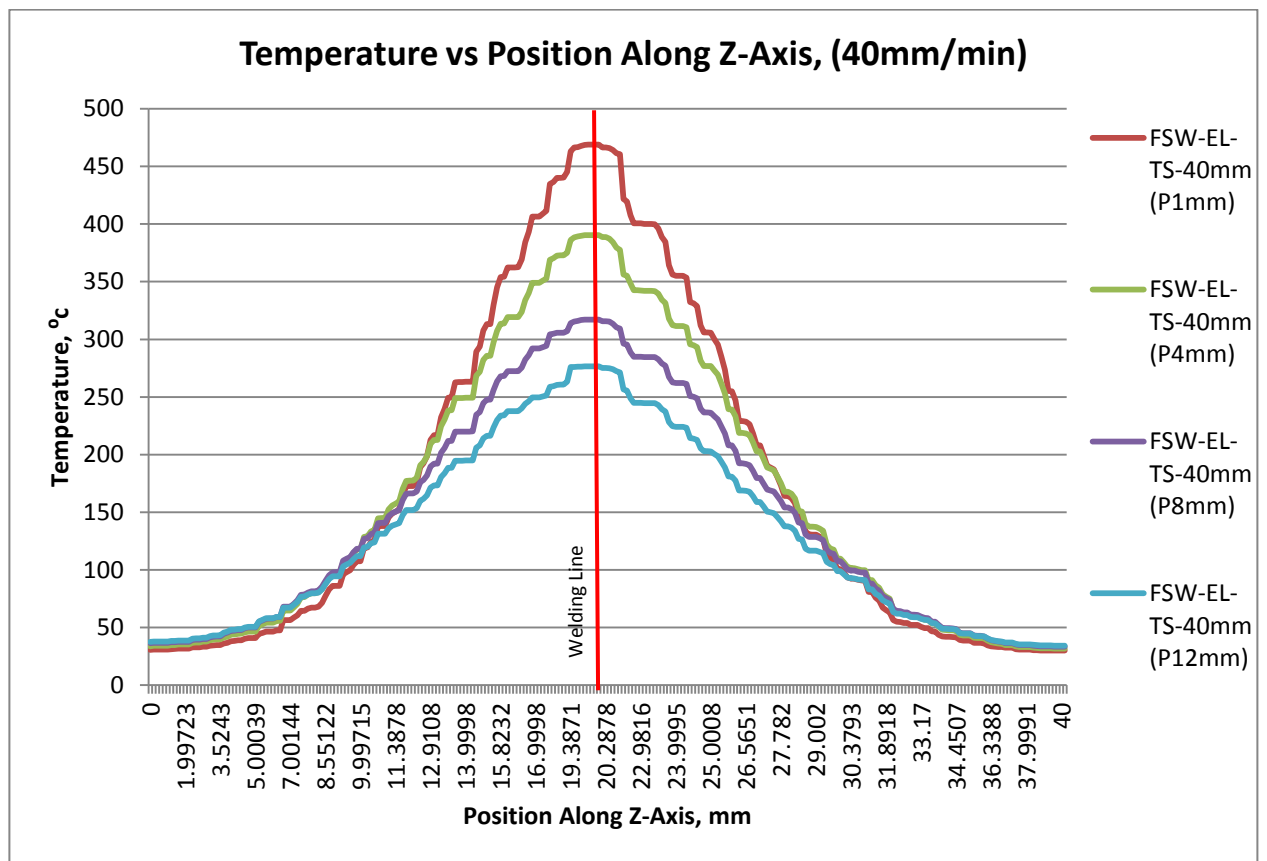


Figure 4.6 Temperature Distribution of FSW Welding (500 rpm, 40 mm/min)

4.4 Result Validation

Temperature distribution was considered as the primary assessment to validate the accuracy of FE analysis on FSW welding. Although the theoretical calculation had been used to verify the model, it was not sufficient to validate the model since the calculation was based on steady-state condition. However, the steady-state temperature was required to assess the validity of the previous researches that were used to verify this simulation.

The figure 4.7 described the temperature distribution of FSW welding on aluminium alloy, AA5083 extracted from Iordache et al. (2016). The welding speed used in the simulation was 40mm/min and the rotational speed was 500rpm. It plotted the temperature obtained from FE analysis and experiment. The peak temperature recorded from the FE analysis was about 425⁰c.

Meanwhile, the peak temperature from this study recorded from the FE simulation of FSW welding with the similar welding parameter was 468.967⁰c. It was higher by 43.967⁰c or about 10.34% which is almost 10%. Therefore, the modelling method used in this project was acceptable. The difference was might due to some parameters that had not been disclosed by the research such as amount of heat energy transferred to the workpiece, axial force and etc.

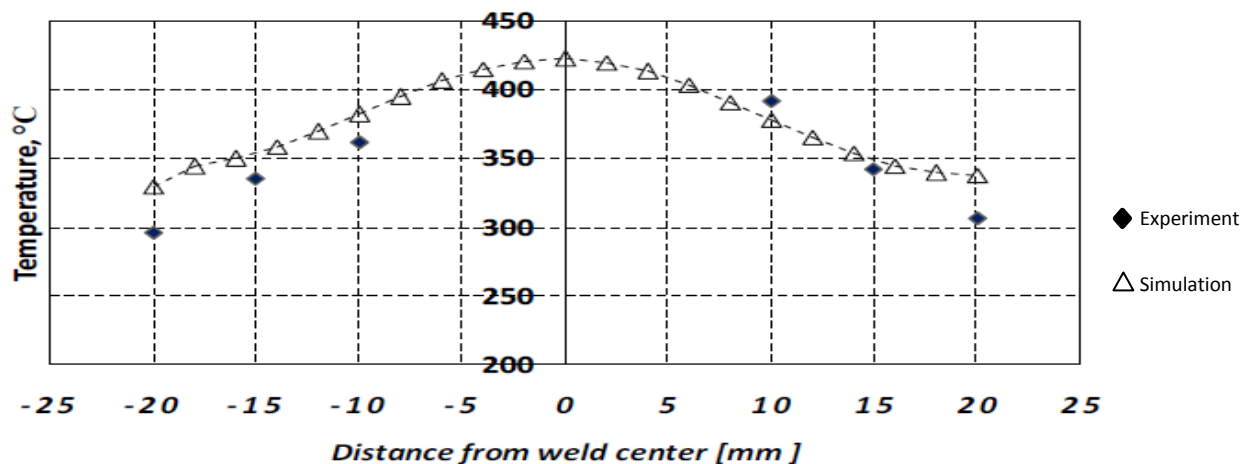


Figure 4.7 Temperature Distribution of FSW Welding of both Simulation and Experimental on aluminium alloy, AA5083 (Welding Speed: 40mm/min, Rotational Speed: 500rpm)

CHAPTER 5

CONCLUSION AND RECOMMENDATION

5.1 Conclusion

Finite Element Analysis (FEA) for friction stir welding could provide more understanding on the behavior of the workpiece during the process. As the main parameter that affects the quality of welded joint is thermal related characteristic, FE analysis has superior advantages compare to experimental approaches. By applying numerical analysis, thermal distribution or even stress distribution in the workpiece can be estimated accurately without using a lot of resources (money and time). However, the FE analysis for FSW can be time consuming process due to its high deformation nature which prevents researches from applying this approach. Thus, it requires numerical analysis using explicit method that could consume a lot of time.

This study has specifically designed to reduce the time required to execute FE analysis on FSW welding using explicit method. It has developed the FSW model based on Coupled Eulerian-Lagrangian method due to its ability to tolerate high material deformation. Three laws have been incorporated in the modelling process; Coupled Eulerian-Lagrangian formulation, Johnson-Cook material law and Coulomb's law of friction. Time scaling has been introduced in the simulation to make the whole process faster.

It can be concluded that time scaling can be used together with Coupled Eulerian-Lagrangian model to simulate FSW process. This approach has been validated with a previous research in which the peak temperature recorded in this study was higher by 10.34%. It is still acceptable since there are some parameters used in their FE analysis have not been disclosed in their researches.

5.2 Recommendation

The study has concluded that time-scaling can be used in Coupled Eulerian-Lagrangian model of FSW welding. There has been no issue when during the model validation based on temperature distribution. However, further study need to be conducted to assess the effect of time-scaling on stress and strain characteristics of the workpiece. Besides that, time-scaling might has the potential to be incorporated with other modelling method such as Arbitrary Lagrangian-Eulerian (ALE) model and Adaptive Remeshing techniques to shorten the time required for analysis. Thus, it requires further study to ensure this approach can be beneficial in producing accurate result.

REFERENCES

1. Journal

Buffa, G., Fratini, L., & Pasta, S. (2009). Residual stresses in friction stir welding: Numerical simulation and experimental verification. *International Centre for Diffraction Data*, 444-452.

Chandrashekar, A., Reddappa, H. N., & Ajaykumar, B. S. (2016). Influence of Tool Profile on Mechanical Properties of Friction Stir Welded Aluminium Alloy 5083. *International Journal of Chemical, Molecular, Nuclear, Materials and Metallurgical Engineering*, **10**(1), 8-14.

El-Sayed, M. M., Shash, A. Y., & Abd-Rabou, M. (2018). Finite element modeling of aluminum alloy AA5083-O friction stir welding process. *Journal of Materials Processing Technology*, **252**, 13-24. doi:10.1016/j.jmatprotec.2017.09.008

El-Sayed, M. M., Shash, A. Y., Mahmoud, T. S., & Rabbou, M. A. (2018). Effect of Friction Stir Welding Parameters on the Peak Temperature and the Mechanical Properties of Aluminum Alloy 5083-O. In *Improved Performance of Materials* (pp. 11-25).

Fei, X., & Wu, Z. (2018). Research of temperature and microstructure in friction stir welding of Q235 steel with laser-assisted heating. *Results in Physics*, **11**, 1048-1051. doi:10.1016/j.rinp.2018.11.039

Frigaard, Grong, & Midling, O. T. (2001). A Process Model for Friction Stir Welding of Age Hardening Aluminum Alloys. *METALLURGICAL AND MATERIALS TRANSACTIONS A*, **32**(5), 1189-1200. doi:10.1007/s11661-001-0128-

Gambirasio, L., & Rizzi, E. (2014). On the calibration strategies of the Johnson–Cook strength model: Discussion and applications to experimental data. *Materials Science and Engineering: A*, **610**, 370-413. doi:10.1016/j.msea.2014.05.006

Grujicic, M., Pandurangan, B., Cheeseman, B. A., & Yen, C. F. (2011). Modifications in the AA5083 Johnson-Cook Material Model for Use in Friction Stir Welding Computational Analyses. *Journal of Materials Engineering and Performance*. doi:10.1007/s11665-011-0118-7

Gupta, A. K., Llyod, D. J., & Court, S. A. (2001). Precipitation hardening processes in an Al–0.4%Mg–1.3%Si–0.25%Fe aluminum alloy. *Materials Science and Engineering*, **A301**, 140-146.

Hasan, A. F. (2019). CFD modelling of friction stir welding (FSW) process of AZ31 magnesium alloy using volume of fluid method. *Journal of Materials Research and Technology*, **8(2)**, 1819-1827. doi:10.1016/j.jmrt.2018.11.016

Iordache, M., Badulescu, C., Iacomì, D., Nitu, E., & Ciuca, C. (2016). Numerical Simulation of the Friction Stir Welding Process Using Coupled Eulerian Lagrangian Method. *IOP Conference Series: Materials Science and Engineering*, **145**. doi:10.1088/1757-899x/145/2/022017

Jannet, S., Mathews, P. K., & Raja, R. (2014). Comparative investigation of friction stir welding and fusion welding of 6061 T6 – 5083 O aluminum alloy based on mechanical properties and microstructure. *Bulletin of the Polish Academy of Sciences Technical Sciences*, **62(4)**, 791-795. doi:10.2478/bpasts-2014-0086

Khodir, S. A., Shibayanagi, T., & Naka, M. (2006). Microstructure and Mechanical Properties of Friction Stir Welded AA2024-T3 Aluminum Alloy. *Materials Transactions*, **47(1)**, 185-193. doi:10.2320/matertrans.47.185

Kiral, B. G., Tabanoglu, M., & Serindag, H. T. (2013). Finite Element Modeling of Friction Stir Welding in Aluminum Alloys Joint. *Mathematical and Computational Applications*, **18**(2), 122-131.

Kundu, J., & Singh, H. (2017). Friction stir welding of AA5083 aluminium alloy: Multi-response optimization using Taguchi-based grey relational analysis. *Advances in Mechanical Engineering*, **8**(11). doi:10.1177/1687814016679277

Lombard, H., Hattingh, D. G., Steuwer, A., & James, M. N. (2009). Effect of process parameters on the residual stresses in AA5083-H321 friction stir welds. *Materials Science and Engineering: A*, **501**(1-2), 119-124. doi:10.1016/j.msea.2008.09.078

Mao, Y., Ke, L., Liu, F., Huang, C., Chen, Y., & Liu, Q. (2015). Effect of welding parameters on microstructure and mechanical properties of friction stir welded joints of 2060 aluminum lithium alloy. *The International Journal of Advanced Manufacturing Technology*, **81**(5-8), 1419-1431. doi:10.1007/s00170-015-7191-2

Meyghani, B., Awang, M., Emamian, S. S., Mohd Nor, M. K., & Pedapati, S. R. (2017). A Comparison of Different Finite Element Methods in the Thermal Analysis of Friction Stir Welding (FSW). *Metals*, **7**(10). doi:10.3390/met7100450

Rashed, A., Yazdani, M., Babaluo, A. A., & Hajizadeh Parvin, P. (2016). Investigation on high-velocity impact performance of multi-layered alumina ceramic armors with polymeric interlayers. *Journal of Composite Materials*, **50**(25), 3561-3576. doi:10.1177/0021998315622982

Sheikh-Ahmad, J. Y., Ali, D. S., Deveci, S., Almaskari, F., & Jarrar, F. (2019). Friction stir welding of high density polyethylene—Carbon black composite. *Journal of Materials Processing Technology*, **264**, 402-413. doi:10.1016/j.jmatprotec.2018.09.033

Summers, P. T., Chen, Y., Rippe, C. M., Allen, B., Mouritz, A. P., Case, S. W., & Lattimer, B. Y. (2015). Overview of aluminum alloy mechanical properties during and after fires. *Fire Science Reviews*, **4**(1). doi:10.1186/s40038-015-0007-5

Thomas, W. M., Johnson, K. I., & Wiesner, C. S. (2003). Friction Stir Welding – Recent Developments in Tool and Process Technologies. *Advanced Engineering Materials*, **5**(7), 485-490. doi:10.1002/adem.200300355

Yaduwanshi, D. K., Bag, S., & Pal, S. (2014). Heat transfer analyses in friction stir welding of aluminium alloy. *Proceedings of the Institution of Mechanical Engineers, Part B: Journal of Engineering Manufacture*, **229**(10), 1722-1733. doi:10.1177/0954405414539297

Yu, H., Zheng, B., & Lai, X. (2018). A modeling study of welding stress induced by friction stir welding. *Journal of Materials Processing Technology*, **254**, 213-220. doi:10.1016/j.jmatprotec.2017.11.022

APPENDICES

Turnitin Similarity Report

FYP 2 - Dissertation Report

ORIGINALITY REPORT

11%

SIMILARITY INDEX

6%

INTERNET SOURCES

7%

PUBLICATIONS

8%

STUDENT PAPERS

PRIMARY SOURCES

1

Submitted to Universiti Teknologi Petronas

Student Paper

2%

2

M.M. El-Sayed, A.Y. Shash, M. Abd-Rabou.
"Finite element modeling of aluminum alloy
AA5083-O friction stir welding process", Journal
of Materials Processing Technology, 2018

Publication

1%

3

e-sciencecentral.org

Internet Source

1%